Growth Activation Alone Is Not Sufficient to Cause Metastatic Thyroid Cancer in a Mouse Model of Follicular Thyroid Carcinoma

Changxue Lu, Li Zhao, Hao Ying, Mark C. Willingham, and Sheue-yann Cheng

Laboratory of Molecular Biology (C.L., L.Z., H.Y., S.C.), Center for Cancer Research, National Cancer Institute, Bethesda, Maryland 20892-4264; and Department of Pathology (M.C.W.), Wake Forest University, Winston-Salem, North Carolina 27157-1072

Downloaded from https://academic.oup.com/endo/article/151/4/1929/2456740 by guest on 20 August 2022

TSH is the major stimulator of thyrocyte proliferation, but its role in thyroid carcinogenesis remains unclear. To address this question, we used a mouse model of follicular thyroid carcinoma (FTC) ($TR\beta^{PV/PV}$ mice). These mice, harboring a dominantly negative mutation (PV) of the thyroid hormone-β receptor (TRβ), exhibit increased serum thyroid hormone and elevated TSH. To eliminate TSH growth-stimulating effect, $TR\beta^{PV/PV}$ mice were crossed with TSH receptor gene knockout ($TSHR^{-/-}$) mice. Wild-type siblings of $TR\beta^{PV/PV}$ mice were treated with an antithyroid agent, propylthiouracil, to elevate serum TSH for evaluating long-term TSH effect (WT-PTU mice). Thyroids from $TR\beta^{PV/PV}TSHR^{-/-}$ showed impaired growth with no occurrence of FTC. Both WT-PTU and $TR\beta^{PV/PV}$ mice displayed enlarged thyroids, but only $TR\beta^{PV/PV}$ mice developed metastatic FTC. Molecular analyses indicate that PV acted, via multiple mechanisms, to activate the integrins-Src-focal adhesion kinase-p38 MAPK pathway and affect cytoskeletal restructuring to increase tumor cell migration and invasion. Thus, growth stimulated by TSH is a prerequisite but not sufficient for metastatic cancer to occur. Additional genetic alterations (such as PV), destined to alter focal adhesion and migration capacities, are required to empower hyperplastic follicular cells to invade and metastasize. These *in vivo* findings provide new insights in understanding carcinogenesis of the human thyroid. **(*Endocrinology* 151: 1929–1939, 2010)**

TSH exerts its action through the binding of its transmembrane receptor, TSHR, to regulate the growth and function of thyroid follicular cells. TSHR null-mice ($TSHR^{-/-}$) exhibit impaired thyroid growth and congenital hypothyroidism that requires an exogenous thyroid hormone supply to maintain the animal's viability (1). Whereas the importance of TSH in follicular proliferation and the function of the adult thyroid gland is certain, less clear is its role in thyroid carcinogenesis. Some studies implied that TSH could act to initiate thyroid carcinogenesis (2), whereas other reports disputed this possibility (3). We therefore decided to study the role of TSH in thyroid carcinogenesis *in vivo* using a mouse model of follicular thyroid cancer ($TR\beta^{PV/PV}$ mice). This mouse model has unique characteristics that make it well suited for use in understanding the role of TSH in cancer development. The $TR\beta^{PV/PV}$ mouse harbors a knock-in dominantly negative mutation of the thyroid hormone β receptor (TRβ) gene, denoted as PV. The PV mutation was identified in a patient with thyroid hormone resistance syndrome (RTH) (4). The cardinal features of RTH are elevated thyroid hormone accompanied by nonsuppressible TSH (5). Thus, the $TR\beta^{PV/PV}$ mouse faithfully reproduces human RTH by exhibiting nonsuppressible highly elevated TSH (6).

As $TR\beta^{PV/PV}$ mice age, they spontaneously develop follicular thyroid carcinoma (FTC) with pathological progression and metastasis patterns and frequency similar to those of human FTC (7). Detailed molecular analyses

ISSN Print 0013-7227 ISSN Online 1945-7170
Printed in U.S.A.
Copyright © 2010 by The Endocrine Society
doi: 10.1210/en.2009-1017 Received September 1, 2009. Accepted December 22, 2009.
First Published Online February 4, 2010

Abbreviations: ATF2, Activating transcription factor; CREB, cAMP response element-binding protein; ECM, extracellular matrix; FAK, focal adhesion kinase; FTC, follicular thyroid carcinoma; Grb2, growth factor receptor binding protein 2; H & E, hematoxylin and eosin; MKK, MAPK kinase; MMP, matrix metalloproteinase; mTOR, mammalian target of rapamycin; PI3K, phosphatidylinositol 3-kinase; PTU, propylthiouracil; RTH, thyroid hormone resistance syndrome; TGFβR1, TGFβ receptor type 1; TRβ, thyroid hormone-β receptor; TSHR, TSH receptor; WT, wild type.

show that altered expression of several genes and signaling pathways during thyroid carcinogenesis of TR$\beta^{PV/PV}$ mice are consistent with those reported for human FTC. For example, similar to human FTC, the phosphatidylinositol 3-kinase (PI3K)-AKT pathway is activated in the thyroid tumors of TR$\beta^{PV/PV}$ mice (8, 9). As in human FTC, the expression of the pituitary tumor-transforming gene is aberrantly activated in TR$\beta^{PV/PV}$ mice (10), leading to aneuploidy and other chromosomal abnormalities (11). Recently consistent with the genetic abnormalities observed in Cowden syndrome, we found that phosphatase and tensin homolog deficiency exacerbates tumor progression of TR$\beta^{PV/PV}$ mice (12). Thus, evidence accumulated so far supports the TR$\beta^{PV/PV}$ mouse as a valid mouse model of FTC.

That the TR$\beta^{PV/PV}$ mice exhibit highly elevated TSH and spontaneous development of FTC has provided an opportunity to clarify the role of TSH in thyroid carcinogenesis. Our approach was to cross TR$\beta^{PV/PV}$ mice with TSHR knockout mice (TSHR$^{-/-}$ mice) to eliminate the effect of TSH-TSHR signaling during carcinogenesis. The effect of TSH-TSHR signaling on thyroid growth and possible cancer development was evaluated using wild-type mice (WT) rendered hypothyroid to elevate serum TSH levels (WT-PTU). Using these mice with or without TSH-TSHR signaling, we found that the thyroid of TR$\beta^{PV/PV}$ mice deficient in TSHR (TR$\beta^{PV/PV}$TSHR$^{-/-}$ mice) had no development defect but exhibited impairment in growth. WT-PTU had a 9.1-fold higher serum TSH level than did TR$\beta^{PV/PV}$ mice, but the extent of thyroid pathology was less than that of TR$\beta^{PV/PV}$ mice at the same age. Importantly, whereas the thyroid tumor cells of TR$\beta^{PV/PV}$ mice exhibited distant metastasis, the hyperplastic follicular cells of WT-PTU mice failed to metastasize to distant sites. Thus, TSH-TSHR signaling stimulates the growth of the thyroid. However, the growth signaling alone is not sufficient to induce metastatic FTC. Additional genetic changes destined to alter extracellular matrix, focal adhesion, and subsequent signaling pathways are obligatory for the development of metastatic FTC. In TR$\beta^{PV/PV}$ mice, the TRβ mutant, PV, via multiple mechanisms, activated integrins, cSrc/focal adhesion kinase, cytoskeletal structures, and p38 MAPK signaling to increase cell motility, migration capacities, and invasion. The present study shows that in FTC, growth and metastasis are two related but independent processes. The former is a prerequisite for the latter to occur. However, without additional genetic alterations to enable the latter to occur, there would be no metastatic carcinoma. Thus, the present study shows that TSH is necessary but not sufficient to cause metastatic follicular thyroid carcinoma in this mouse model.

Materials and Methods

Animals

The animal protocols used in the present study were approved by the National Cancer Institute Animal Care and Use Committee. TSHR knockout mice (TSHR$^{-/-}$ mice) were generously provided by Dr. Terry F. Davies (1). TR$\beta^{PV/+}$ (6) and TSHR$^{+/-}$ mice were crossed to generate TR$\beta^{+/+}$TSHR$^{+/+}$ (WT mice), TR$\beta^{+/+}$TSHR$^{-/-}$, TR$\beta^{PV/PV}$TSHR$^{+/+}$(TR$\beta^{PV/PV}$ mice), and TR$\beta^{PV/PV}$TSHR$^{-/-}$ for analysis. The diet for TSHR$^{-/-}$ mice was Pico Rodent Chow-20 supplemented with 100 ppm desiccated thyroid powder (T100) (Testdiet, Purina Mills, Gray Summit, MO), given *ad libitum* to maintain thyroid hormone levels. To generate mice with a high TSH level, WT siblings of TR$\beta^{PV/PV}$ mice were fed with an iodine-deficient diet supplemented with 0.15% propylthiouracil (PTU) (Harlan Teklab, Indianapolis, IN) *ad libitum* starting at the age of 2 months.

Hormone assays

Serum levels of total T_3 and total T_4 were determined by using a GammaCoat T_4 or T_3 assay RIA kit (DiaSorin, Stillwater, MN) according to the manufacturer's instructions. Serum TSH levels were measured as previously described (6).

Histopathological analysis and immunohistochemistry

Thyroid glands and lungs were dissected, fixed in 10% neutral buffered formalin (Sigma-Aldrich, St. Louis, MO), and subsequently embedded in paraffin. Five-micrometer-thick sections were stained with hematoxylin and eosin (H & E) and analyzed. Immunohistochemistry was performed as previously described (6) with some modifications. For antigen retrieval step, slides were heated in 0.05% citraconic anhydride solution (Sigma-Aldrich) (pH 7.4) at 98 C for 45 min followed by treatment with rabbit anti-Ki67 (1:50 dilution, NeoMarker; Thermo Scientific, Swedesboro, NJ) at 4 C overnight. The antigen signals were detected by treatment with peroxidase substrate diaminobenzidine followed by counterstaining with Gill's hematoxylin.

Western blot analysis and coimmunoprecipitation

Twenty to thirty micrograms of thyroid lysate prepared similarly as described previously (13) were analyzed for protein abundance by Western blot analysis. The antibodies for p-AKT (1:500 dilution), total AKT (1:1000 dilution), p-p38 MAPK (1:500 dilution), total p38 MAPK (1:1000 dilution), phosphorylated MAPK kinase (MKK)-3/6 (1:500 dilution), total MKK6 (1:500 dilution), phosphorylated activating transcription factor 2 (ATF2; 1:500 dilution), total ATF2 (1:500 dilution), β-actin (1:1000 dilution), and glyceraldehyde-3-phosphate dehydrogenase (1:1000) were purchased from Cell Signaling Technology (Danvers, MA). Antibodies for integrin αV, integrin α5, integrin β3, integrin β1, cyclin D1, growth factor receptor binding protein 2 (Grb2) (all at 1:200 dilution), TGFβ1, and total focal adhesion kinase (FAK; 1:250 dilution) were purchased from Santa Cruz Biotechnology (Santa Cruz, CA). Ezrin antibody (1:500 dilution) was purchased from Upstate Biotechnology (Lake Placid, NY). Antibodies for pFAK-Y397, -Y407, and -Y576 (all in 1:250 dilution) were from BioSource (Invitrogen, Carlsbad, CA). For coimmunoprecipitation, 1.5 mg of thyroid lysates were immunoprecipitated with 4 μg polyclonal anti-TRβ-A/B domain

Downloaded from https://academic.oup.com/endo/article/151/4/1929/2456740 by guest on 20 August 2022

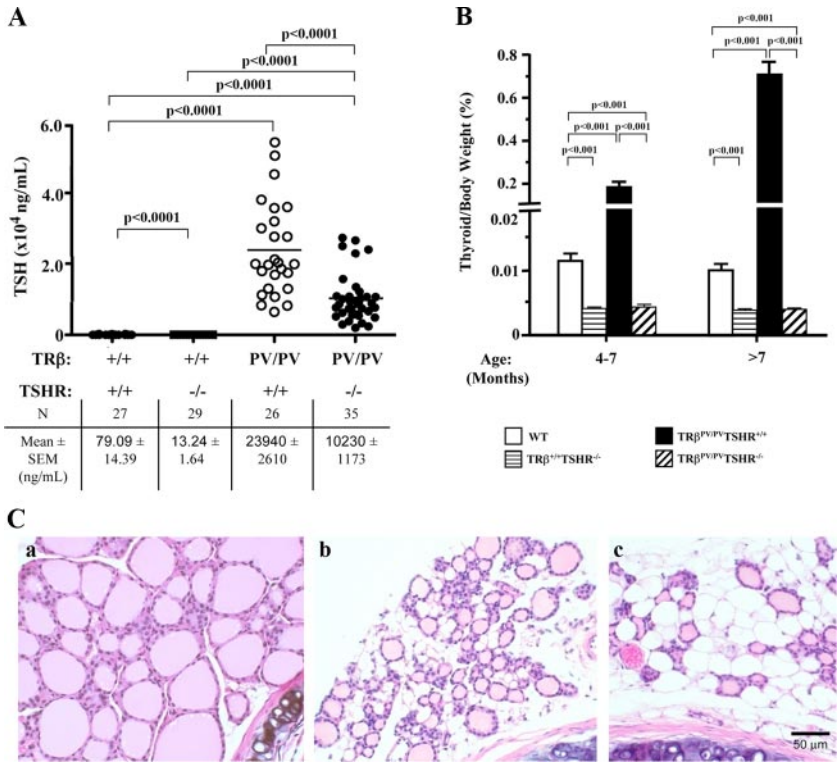

FIG. 1. Comparison of serum TSH levels (A) (number of mice, N, as shown; age 5–12 months) and thyroid weight (B) among mice with genotypes indicated. Data are expressed as mean values ± SEM with *P* values shown. Sample sizes (N) for thyroid weight analysis (B) in different groups are in the younger age group (4–7 months), n = 8, 17, 6, and 13 for WT, TR$\beta^{+/+}$TSHR$^{-/-}$, TR$\beta^{PV/PV}$TSHR$^{+/+}$, and TR$\beta^{PV/PV}$TSHR$^{-/-}$ mice, respectively; in the older age group (>7 months), n = 8, 26, 11, and 9 for above-mentioned four groups, respectively. C, H & E-stained thyroids from WT (a), TR$\beta^{+/+}$TSHR$^{-/-}$ (b), or TR$\beta^{PV/PV}$TSHR$^{-/-}$ mice (c) (aged 6–8 months).

antibody (Rockland Immunochemicals, Gilbertsville, PA), mouse monoclonal anti-TRβPV antibody (no. 302), normal rabbit IgG, or mouse IgG. Bound proteins were analyzed by Western blot using the specific antibodies denoted in the figures.

Quantitative RT-PCR

Total RNA (200 ng) of thyroids, prepared by using TRIzol (Invitrogen) according to the manufacturer's instructions, was used for quantitative RT-PCR. The specific primers for detection of various genes are shown in Supplemental Table 1 published on The Endocrine Society's Journals Online web site at http://endo.endojournals.org.

Statistical analysis

All data are expressed as the mean ± SEM. Statistical analysis was performed with the Student's *t* test, and $P < 0.05$ was considered significant by using StatView 5.0 (Abacus Concepts, Inc., San Diego, CA).

Results

Impaired thyroid growth in TR$\beta^{PV/PV}$ mice deficient in TSH receptors

To block TSH action, TR$\beta^{PV/PV}$ mice were crossed with TSHR$^{-/-}$ mice (1) and spontaneous thyroid carcinogenesis in the offspring was monitored. In the presence of TSHR, serum TSH concentrations in TR$\beta^{PV/PV}$TSHR$^{+/+}$ mice (hereafter simply denoted as TR$\beta^{PV/PV}$ mice) were 303-fold higher than in WT mice, which are similar to values previously reported (Fig. 1A) (6). In TR$\beta^{PV/PV}$TSHR$^{-/-}$ mice, serum TSH levels were 58% lower than that in TR$\beta^{PV/PV}$ mice. No age-dependent changes in TSH levels were observed up to 12 months of age. Thyroid hormones supplemented in the chow could maintain T_3 and T_4 levels in TR$\beta^{+/+}$TSHR$^{-/-}$ mice such that they were not significantly different from those in WT mice (data not shown); the serum TSH concentrations in TR$\beta^{+/+}$TSHR$^{-/-}$ mice were 6.1-fold lower than those in WT mice (Fig. 1A). Compared with WT mice, the serum total T_3 and T_4 concentrations of TR$\beta^{PV/PV}$TSHR$^{-/-}$ mice were only slightly elevated (1.4- and 2.9-fold, respectively) but were 6.7- and 4.8-fold, respectively, lower than those of TR$\beta^{PV/PV}$ mice (data not shown).

Figure 1B compares thyroid weights among WT, TR$\beta^{+/+}$TSHR$^{-/-}$, TR$\beta^{PV/PV}$ mice, and TR$\beta^{PV/PV}$TSHR$^{-/-}$ mice by age. The thyroid weight of TR$\beta^{PV/PV}$ mice was 9- and 62-fold increase as compared with WT mice at age 4–7 and older than 7 months, respectively. The effect of the loss of TSHR was evident as the thyroid weight of TR$\beta^{+/+}$TSHR$^{-/-}$ and TR$\beta^{PV/PV}$TSHR$^{-/-}$ mice was less than half of that in WT mice at the two age groups (Fig. 1B). Consistent with the reduced thyroid growth, histological assessment indicates that compared with the WT thyroid (Fig. 1Ca), smaller follicles were observed in the thyroid of TR$\beta^{+/+}$ TSHR$^{-/-}$ mice (Fig. 1Cb) as well as in TR$\beta^{PV/PV}$TSHR$^{-/-}$ mice (Fig. 1Cc).

TSH is necessary, but not sufficient, to induce metastatic follicular thyroid carcinoma

To understand the role of TSH in thyroid carcinogenesis, we treated WT mice with PTU (WT-PTU), beginning at the age of 2 months, for more than a year. This treatment led to a remarkably elevated serum TSH concentration (127,514.25 ± 14,887 ng/ml, n = 31) that was 9.1-fold higher than in TR$\beta^{PV/PV}$ mice (Fig. 2A). Figure 2B shows the thyroid weight of TR$\beta^{PV/PV}$ mice was 9- and 62-fold increase as compared with WT mice at age 4–7 and older than 7 months, respectively; the thyroid weight of WT-PTU was 4- and 16-fold increased as compared with WT mice, respec-

Downloaded from https://academic.oup.com/endo/article/151/4/1929/2456740 by guest on 20 August 2022

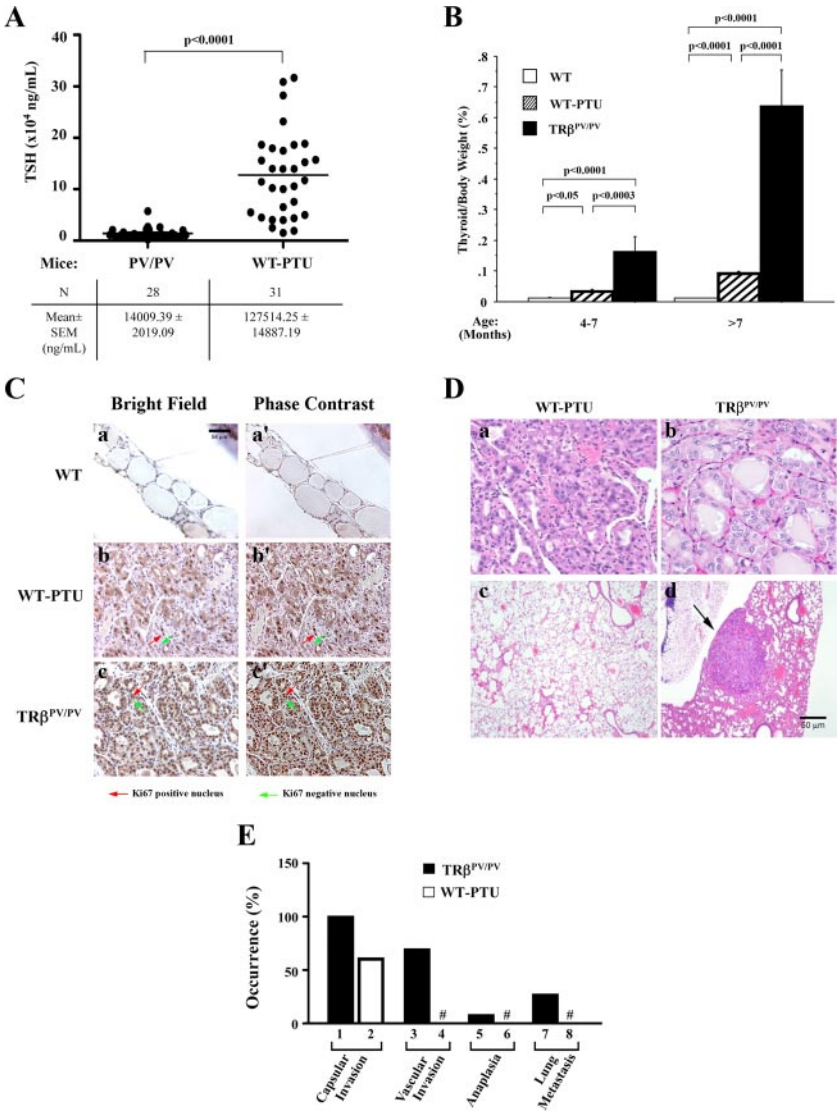

FIG. 2. Comparison of serum TSH levels (A) (N as shown) and thyroid weight (B) among mice with indicated genotypes. Data are expressed as mean values ± SEM with *P* values indicated. Sample sizes (N) in thyroid weight calculation (B) for different groups are in the younger age group (4–7 months), n = 13, 5, and 7 for WT, WT-PTU, and TR$\beta^{PV/PV}$ mice, respectively; in older age group (>7 months), n = 20, 31, and 11 for above-mentioned three groups, respectively. C, The immunohistochemical analysis of Ki67 in thyroids from mice (aged 10–12 months) with indicated genotypes. To clearly display the unlabeled thyrocytes, phase-contrast images (panels a′–c′) were presented here in parallel to bright-field images (a–c). The *red arrows* indicate Ki67-labeled nuclei, whereas the *green arrows* show nonreactive nuclei in thyroids. D, H & E-stained thyroid cells (a) and lung (c) of WT-PTU mice, thyroid cells (b), and lung (d) of TR$\beta^{PV/PV}$ mice. E, Comparison of frequency occurrence of pathological features between TR$\beta^{PV/PV}$ (n = 50) and WT-PTU mice (n = 25). #, Zero occurrence.

tively. Thus, the thyroid weight of WT-PTU was 4-fold lower than that of TR$\beta^{PV/PV}$ mice at 4–7 months and 7-fold lower in mice older than 7 months despite a higher TSH level in WT-PTU mice than in TR$\beta^{PV/PV}$ mice (Fig. 2A). These results indicate that in TR$\beta^{PV/PV}$ mice, the growth of the thyroid was not only stimulated by the TSH/TSHR signaling but also by additional PV-mediated stimulatory effects. These results suggested that PV, collaborating with TSH/TSHR signaling, further promotes thyrocyte proliferation.

That thyrocytes of TR$\beta^{PV/PV}$ mice had increased proliferation as compared with those of WT-PTU mice was evident by Ki67 nuclear staining (Fig. 2C). Analysis of immunostained thyroids of WT, WT-PTU, and TR$\beta^{PV/PV}$ mice revealed that the majority of nuclei in thyroid epithelial cells in TR$\beta^{PV/PV}$ mice labeled strongly with anti-Ki67 antibodies (*red arrows*; Fig. 2C, c and c′), indicating that they were actively in the cell cycle. In contrast, thyroids from WT-PTU mice showed that only a subset (~50%) of epithelial cells were in the cell cycle (Fig. 2C, b and b′), whereas the WT untreated animals showed only a very small fraction (5%) of thyroid epithelial cells actively in the cell cycle. The sections were viewed both routinely by bright-field microscopy (Fig. 2C, a–c) and phase-contrast microscopy (Fig. 2C, a′, b′, and c′); phase contrast enhanced the detection of the peroxidase reaction product (*red arrows*).

That PV had additional effects on thyrocytes of TR$\beta^{PV/PV}$ mice in addition to TSH-mediated growth was made evident by histopathological analysis. Figure 2Da shows that the number of hyperplastic follicular cells of WT-PTU increased but their nuclear size was only slightly increased as compared with that of normal thyrocytes (see Fig. 1Ca). In contrast, the nuclei of hyperplastic follicular cells of TR$\beta^{PV/PV}$ mice showed an increase in size with clearly more nuclear pleomorphism, characteristics more typical of further neoplastic progression (Fig. 2Db) and indicative of effects of PV beyond proliferation mediated by TSH, as seen in WT-PTU mice.

The pathological progression of thyroids in WT-PTU and TR$\beta^{PV/PV}$ mice was monitored as the animals aged. Figure 2E shows that in mice older than 11 months, 100, 70, 8, and 27% of TR$\beta^{PV/PV}$ mice developed capsular invasion, vascular invasion, anaplasia, and lung metastasis, respectively (an example is shown in Fig. 2Dd). In WT-PTU mice, however, capsular invasion was observed at a lower frequency (60%) but importantly without detectable vascular invasion, anaplasia, and lung metastasis (Fig. 2E). These results indicate that TSH is necessary for aberrant thyroid growth but not sufficient for metastatic FTC to occur.

Downloaded from https://academic.oup.com/endo/article/151/4/1929/2456740 by guest on 20 August 2022

PV collaborates with TSH/TSHR signaling to stimulate thyroid growth via activation of the AKT-mammalian target of rapamycin (mTOR)-p70^{S6K} pathway

The classical TSH-TSHR signaling to stimulate thyrocyte proliferation is via the protein kinase A (PKA)-phosphorylated cAMP response element-binding protein (CREB)-cyclin D1 pathway (14). Indeed, we found a similarly elevated cyclin D1 in the thyroid of TR$\beta^{PV/PV}$ mice and WT-PTU mice, as compared with WT (Fig. 3Aa). These results indicate that consistent with highly elevated serum TSH levels in TR$\beta^{PV/PV}$ and WT-PTU mice, TSH-TSHR-phosphorylated CREB-cyclin D1 signaling is one of the proliferation pathways for thyrocyte proliferation in these mice. However, the finding that thyroid growth in TR$\beta^{PV/PV}$ mice was 4- to 7-fold higher than that of WT-PTU mice (Fig. 2B), despite 9.1-fold higher serum TSH levels in WT-PTU mice than TR$\beta^{PV/PV}$ mice suggests that PV could act on additional pathways to drive thyroid growth. We have shown previously that PV, via physical interaction with the p85α subunit, activates the PI3K-AKT-mTOR-p70^{S6K} pathway to promote growth (8). The finding that the PI3K-AKT-mTOR pathway is regulated by TSH (15, 16) raised the possibility that the TSH- and PV-induced growth-stimulatory signals could converge on this pathway. Indeed, consistent with our previous findings, AKT, mTOR, and p70^{S6K} were activated as indicated by increased phosphorylation (~3-fold; lanes 3 and 4, Fig. 3Ba, c, and e, respectively) as compared with WT mice (lanes 1 and 2) without significantly alteration of the total AKT, mTOR, and p70^{S6K} protein levels (Fig. 3Bb, d, and f, respectively). The phosphorylation of AKT, mTOR, and p70^{S6K} was increased in WT-PTU mice (lanes 5 and 6), but the extent of the increase was lower than that in TR$\beta^{PV/PV}$ mice (~2-fold; Fig. 3B). These results indicate that TSH can stimulate thyroid growth, not only via the classical pathway of PKA-CREB-cyclin D1 but also via the AKT-mTOR-p70^{S6K} pathway. Importantly, PV collaborates with TSH-TSHR signaling to further potentiate the PI3K-AKT-mTOR-p70^{S6K} pathway to promote thyroid growth.

Activation of integrin-mediated signaling in the thyroid of TR$\beta^{PV/PV}$ mice

That TR$\beta^{PV/PV}$ mice, but not WT-PTU mice, exhibited metastatic FTC prompted us to examine key regulators in adhesion, cell migration, and invasion. Several studies

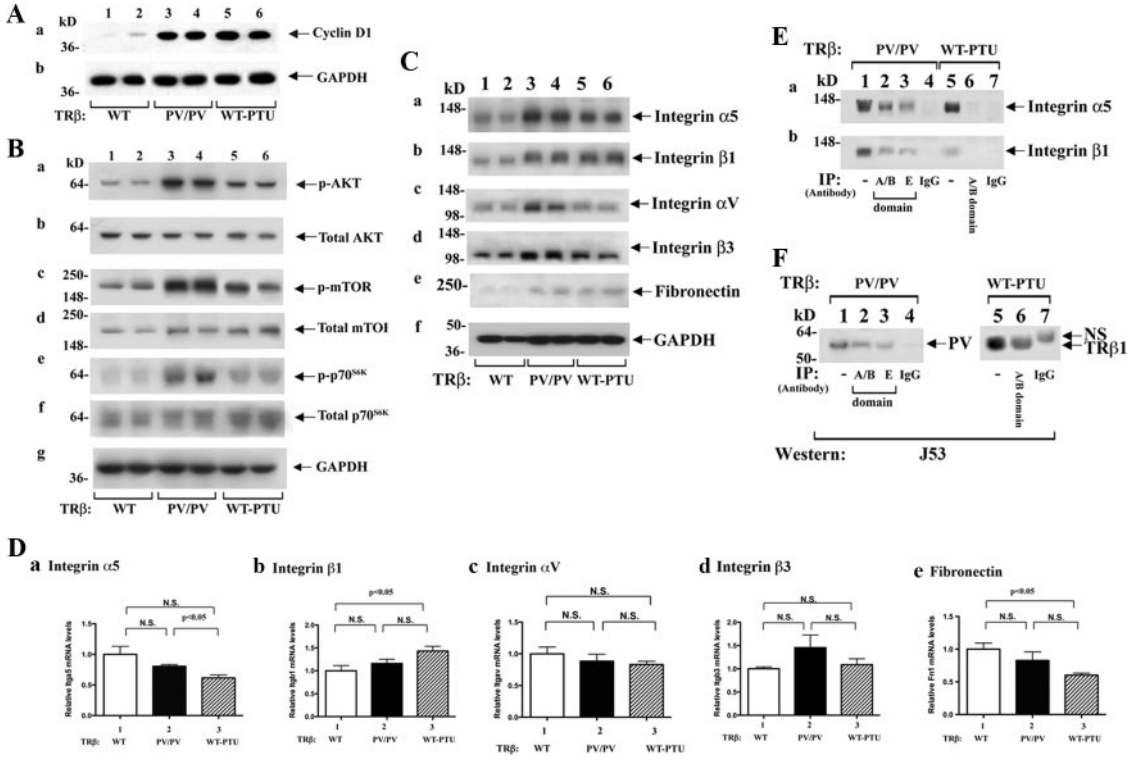

FIG. 3. PV collaborates with TSH-TSHR signaling to stimulate thyroid growth via activating the PI3K-AKT-mTOR-p70^{S6K} signaling pathway (A and B). C, Protein abundance of integrins and fibronectin in WT, TR$\beta^{PV/PV}$, and WT-PTU mice by Western blot analysis. In each assay, 30 μg of thyroid extracts from every mouse genotype were used. Two representative results from four to six WT (lanes 1 and 2), TR$\beta^{PV/PV}$ (lanes 3 and 4), and WT-PTU (lanes 5 and 6) mice are shown. D, Gene expression profiles of integrins (*Itga5*, *Itgb1*, *Itgav*, *Itgb3*) and fibronectin (*Fn1*) in WT, TR$\beta^{PV/PV}$, and WT-PTU mice were determined by real-time RT-PCR. Total RNA from five to six mouse thyroids per each group was prepared as described in *Materials and Methods*. Results are presented as fold change to the mRNA level of WT mice. N.S., Not significant. E, Association of PV with integrins α5 and β1 was demonstrated by coimmunoprecipitation. Lanes 1 and 5 are direct Western blot analysis showing the input of integrin α5 (a), and integrin β1 (b). F, The endogenous TRβ1 or TRβPV protein after immunoprecipitation was detected by immunoblotting with mouse IgM anti-TRβ1-A/B domain antibody (J53). NS, Nonspecific.

Downloaded from https://academic.oup.com/endo/article/151/4/1929/2456740 by guest on 20 August 2022

have shown a close association of altered expression of integrins with acquisition of invasiveness of thyroid cancer (17–20). Integrins are a large family of heterodimeric transmembrane glycoproteins consisting of noncovalently associated α- and β-subunits that regulate cell-cell interaction, migration, proliferation, and angiogenesis (21). We therefore tested the possibility that PV could selectively activate integrin signaling to promote metastasis. We first focused on the integrins $\alpha v\beta 3$ and $\alpha 5\beta 1$ previously shown to affect proliferation and invasiveness of thyroid cells (19, 20). Figure 3C, lanes 3 and 4, shows that the protein levels of $\alpha 5$ (Fig. 3Ca) and $\beta 1$ (Fig. 3Cb) were similarly increased in the thyroids of TR$\beta^{PV/PV}$ and WT-PTU mice compared with those of WT mice, suggesting a common response to the elevated TSH in TR$\beta^{PV/PV}$ and WT-PTU mice. In contrast, lanes 3 and 4 show that αV (Fig. 3Cc) and $\beta 3$ (Fig. 3Cd) were selectively activated in TR$\beta^{PV/PV}$ mice but not in WT-PTU mice. Determination of the protein abundance of the common ligand of integrins $\alpha V\beta 3$ and $\alpha 5\beta 1$, fibronectin, shows that fibronectin abundance was increased in TR$\beta^{PV/PV}$ and WT-PTU mice, as compared with the WT mice (Fig. 3Ce). These results suggested that PV could activate integrin-fibronectin signaling pathways in TR$\beta^{PV/PV}$ mice. However, the majority of the changes in the protein abundance of integrins and fibronectin shown in Fig. 3C was not mediated via transcriptional regulation. As shown in Fig. 3D, a 20–30% reduction in the expression of integrin $\alpha 5$ (Fig. 3Da) and fibronectin (Fig. 3De) mRNA in the thyroid of WT-PTU was observed as compared with TR$\beta^{PV/PV}$ mice and WT- mice, respectively. A small increase of $\beta 1$ in WT-PTU was observed (Fig. 3Db). However no significant alterations of mRNA expression of other integrins were detected (Fig. 3Db and Dd).

The activity of integrins is modulated by interaction with other membrane and/or cytoplasmic proteins. Because TR$\beta^{PV/PV}$ mice, but not WT-PTU mice, exhibit metastasis, we further considered the possibility that PV could physically interact with integrins to stimulate their activity in addition to increase their protein abundance. PV coimmunoprecipitated with integrin $\alpha 5$ when the anti-A/B domain of TR$\beta 1$ antibody was used because PV shares identical A/B domain (Fig. 3Ea, lane 2). The association of PV with integrin $\alpha 5$ was further confirmed by using anticarboxyl terminal PV-mutated sequence antibody (lane 3, specific antibody against PV sequence). The detection of integrin $\alpha 5$ in lanes 2 and 3 was specific because no signals were detected when a control IgG antibody was used (lane 4). In contrast, when anti-A/B domain (lane 6) antibodies were used in immunoprecipitation of thyroid extracts from WT-PTU mice, no signal was observed. Lanes 1 and 5 were from direct Western blot analysis of thyroid extracts in the detection of integrin $\alpha 5$ as positive controls. Similar coimmunoprecipitation experiments also showed that PV was associated with integrin $\beta 1$ (Fig. 3Eb, lanes 2 and 3), but no integrin $\beta 1$ signals were detected in WT-PTU mice (lane 6). However, we did not find an association of PV with integrin αV or $\beta 3$ or fibronectin (data not shown). Figure 3F shows the endogenous PV in the thyroid of TR$\beta^{PV/PV}$ mice (lanes 2 and 3) and TR$\beta 1$ from WT-PTU mice (lane 6). These results indicate that PV selectively associated with integrins $\alpha 5$ and $\beta 1$, and this physical interaction could lead to the activation of integrin signaling in TR$\beta^{PV/PV}$ mice.

Studies in the past decades indicated that cSrc proteins, complexed with FAK affect cell adhesion, invasion, and motility that contribute to tumor progression and metastasis (22). They act to integrate signals initiated from integrin heterodimers and some growth factor receptors to regulate a number of downstream signals to affect cell migration and invasion (22, 23). We therefore determined whether cSrc was activated by autophosphorylation at Y416. Figure 4Aa shows that cSrc was activated in the thyroid of TR$\beta^{PV/PV}$ mice (lanes 3 and 4) but not in WT-PTU mice (lanes 5 and 6), as compared with WT mice (lanes 1 and 2). However, the abundance of total cSrc proteins was not significantly affected (Fig. 4Ab). Lanes 3 and 4 (Fig. 4Ac) show that FAK was also activated by increased autophosphorylation at Y397 in the thyroid of TR$\beta^{PV/PV}$ mice but not in WT-PTU mice, as compared with WT mice (Fig. 4A, lanes 1 and 2). It is important to point out that FAK is the substrate of cSrc and that p-Y397 is the high-affinity binding site for the SH2 domain of cSrc, which, in turn, phosphorylates FAK on a number of additional tyrosine sites. Indeed, consistent with the activation of cSrc, phosphorylation of Y576 and Y407 of FAK was also detected (Fig. 4A, d and e, lanes 3 and 4,). The activation of FAK by increased phosphorylation at Y576 and Y407 was reported to result in increasing cell angiogenesis and motility, respectively (22). In addition to integrins, FAK is also activated by growth factors, such as TGFβ. FAK, once activated, serves as a binding site for the Grb2 (22, 24). Figure 4Ag shows that Grb2 protein abundance was markedly elevated (lanes 3 and 4) in TR$\beta^{PV/PV}$, as compared with WT (lanes 1 and 2) and WT-PTU (lanes 5 and 6) mice. However, this elevated protein abundance of Grb2 was not due to increased transcription as no changes in the mRNA levels were observed (Fig. 4E).

Because it is known that integrins, Grb2, and FAK form complexes on cell membrane (25), we further determined whether FAK was associated with PV by coimmunoprecipitation. Figure 4B shows that FAK was detected when thyroid extracts of TR$\beta^{PV/PV}$ mice were immunoprecipitated with anti-A/B domain of TRβ antibody (lane 2) as

Downloaded from https://academic.oup.com/endo/article/151/4/1929/2456740 by guest on 20 August 2022

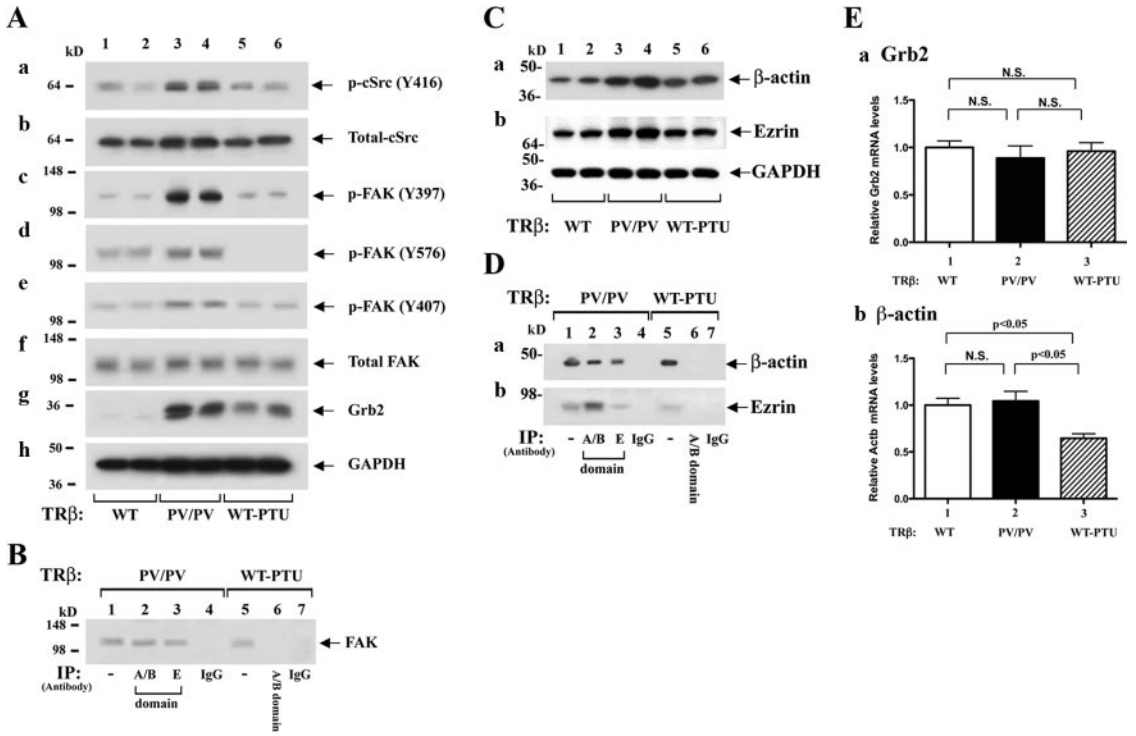

FIG. 4. Increased activation of cSrc-FAK signaling (A) and elevated protein levels of β-actin and ezrin (C) in TRβ$^{PV/PV}$ mice but not WT-PTU mice. For Western blot analysis (A and C), 25 μg of thyroid extracts were used. Two representative results from four to six WT (lanes 1 and 2), TRβ$^{PV/PV}$ (lanes 3 and 4), and WT-PTU (lanes 5 and 6) mice are shown. The proteins analyzed are marked. PV complexing with FAK (B) and β-actin and ezrin (D) was determined by coimmunoprecipitation similarly as described above. Lanes 4 and 7 are the negative controls using IgG for immunoprecipitation (IP; B and D). (E) The mRNA expression profiles of Grb2 (*Grb2*) or β-actin gene (*Actb*) in thyroids of WT, TRβ$^{PV/PV}$, and WT-PTU mice were determined by real-time RT-PCR. Total RNA from five to six mouse thyroids per each group was prepared, and results are presented as fold change to the mRNA level of WT mice. Data are expressed as mean values ± SEM with *P* values indicated. N.S., Not significant.

well as anti-PV-specific antibody (lane 3). But no signals were detected in the extracts of WT-PTU mice (lane 6). Lanes 1 and 5 were obtained by direct Western blot analysis only as positive controls. Therefore, PV was found to associate with the integrins-α5 and -β1 and the FAK complexes (Figs. 3E and 4B).

The activation of cSrc-FAK is known to remodel the actin cytoskeleton in cancer cells that could underlie aberrant cell migration and invasion (26, 27). We therefore determined whether PV induced an altered expression of β-actin at the protein level. Indeed, β-actin abundance was elevated in TRβ$^{PV/PV}$ (Fig. 4Ca, lanes 3 and 4) as well as WT-PTU mice (lanes 5 and 6) but with a lesser extent as compared with WT mice. Interestingly, in contrast to elevated protein abundance, the β-actin mRNA was about 30% lower in WT-PTU as compared with WT and TRβ$^{PV/PV}$ mice (Fig. 4Eb). We also analyzed the protein abundance of ezrin, which cross-links the cytoskeleton and plasma membrane and is involved in the growth and metastatic potential of cancer cells (28). Western blot analysis shows that ezrin abundance was increased in TRβ$^{PV/PV}$ mice (Fig. 4Cb, lanes 3 and 4) but not in WT-PTU mice (lanes 5 and 6), as compared with WT mice (lanes 1 and 2). We further probed whether β-actin and ezrin were part of the PV-α5β1-FAK complexes (see Figs. 3E and 4B). Figure 4D shows that β-actin coimmunoprecipitated with PV in TRβ$^{PV/PV}$ mice (Fig. 4Da, lanes 2 and 3) but not in WT-PTU mic, because when anti-A/B domain antibodies (antigenic sites shared by TRβ and PV) were used, no signals were detected (Fig. 4Da, lane 6). Lanes 1 and 5 show that β-actin and ezrin were detected directly by Western blot analysis. Similarly, ezrin was also found to associate with PV (Fig. 4Db, lanes 2 and 3). These results indicate that PV, by association with integrin α5β1, and β-actin-ezrin transduced the signals from extracellular matrix (ECM)-integrins to alter actin-ezrin-cytoskeletal dynamics to affect cell migration and motility.

Activation of p38 MAPK signaling pathway in the thyroid of TRβ$^{PV/PV}$ but not WT-PTU mice

The activation of p38 MAPK signaling by integrins and cSrc has recently been reported (29). The observations that cSrc and FAK activity were increased in the thyroid of TRβ$^{PV/PV}$ mice prompted us to examine whether the MAPK signaling is one of the downstream pathways that could lead to increased cell invasion and migration. Indeed, Western blot analysis shows the increased phosphorylation of MKK-6 (Fig. 5Aa, lanes 3 and 4) and p38 MAPK in TRβ$^{PV/PV}$ mice (Fig. 5Ac, lanes 3 and 4) but not WT-PTU mice (Fig. 5A, a and c, lanes 5 and 6), as com-

Downloaded from https://academic.oup.com/endo/article/151/4/1929/2456740 by guest on 20 August 2022

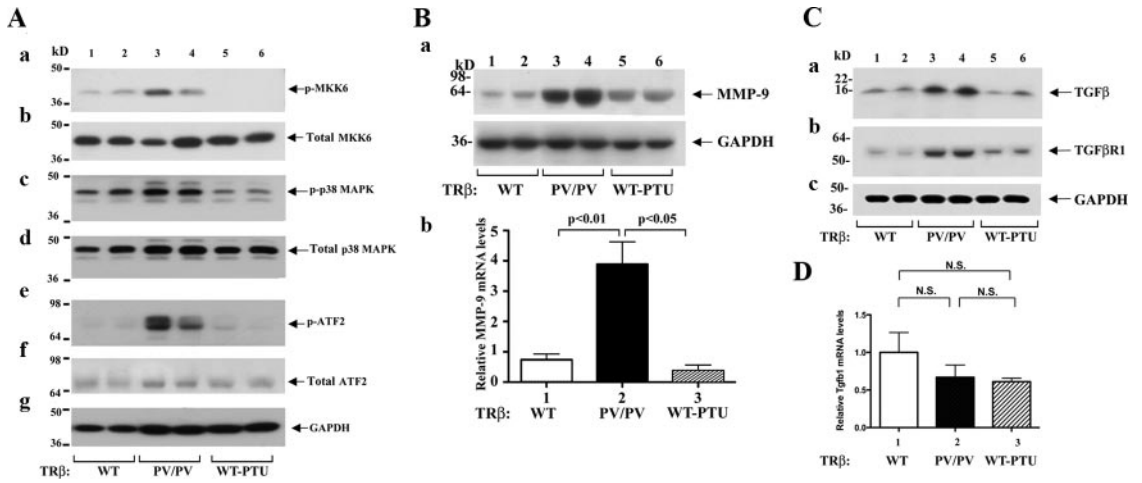

FIG. 5. Activation of p38 MAPK signaling pathway in the thyroid of TR$\beta^{PV/PV}$ mice but not in WT-PTU mice. A, Thyroid extract (30 μg) was used in the Western blot analysis, as described in *Materials and Methods*. The effectors analyzed in the p38 MAPK phosphorylation cascade are marked. Two representative results from five to seven WT (lanes 1 and 2), TR$\beta^{PV/PV}$ (lanes 3 and 4), and WT-PTU (lanes 5 and 6) mice are shown. B, Increased expression of MMP-9 in TR$\beta^{PV/PV}$ mice, but not in WT-PTU mice, at the protein level (a) as well as the mRNA level (b). C, Increased protein levels of TGFβ and TGFβR1 in thyroids of WT, TR$\beta^{PV/PV}$, and WT-PTU mice determined by Western blot analysis. Thirty micrograms of thyroid extract were used and two representative results from four to six WT (lanes 1 and 2), TR$\beta^{PV/PV}$ (lanes 3 and 4), and WT-PTU (lanes 5 and 6) mice are shown. D, The expression of TGFβ gene (*Tgfb1*) mRNA was not significantly different in thyroids of WT, TR$\beta^{PV/PV}$, and WT-PTU mice. Total RNA from five to six mouse thyroids per each group was analyzed by RT-PCR and results are shown as fold change to that of WT mice. N.S., Not significant.

pared with WT-mice (lanes 1 and 2). The increased phosphorylation of MKK6 and p38 MAPK was not due to an increase in the expression of these two kinases because total MKK6 and p38 MAPK protein levels were not significantly different among WT, TR$\beta^{PV/PV}$, and WT-PTU mice (Fig. 5A, b and d). The activation of MKK6-p38 MAPK signaling led to an increase in the phosphorylation of the ATF2 in the thyroid of TR$\beta^{PV/PV}$ mice (Fig. 5Ae, lanes 3 and 4) without affecting the total ATF2 protein levels (Fig. 5Af). Figure 5Ag was the corresponding loading control.

Recent studies indicated that activation of p38 MAPK-ATF2 signaling results in increased expression of matrix metalloproteinases (MMPs) (*e.g.* MMP-9) to induce cell invasion and migration (30, 31). We therefore assessed whether MMP-9 was activated in the thyroid of TR$\beta^{PV/PV}$ mice that exhibit lung metastasis. Western blot analysis shows the MMP-9 protein level was increased 3- to 4-fold (Fig. 5Ba, lanes 3 and 4), as compared with WT-PTU (lanes 5 and 6) and WT (lanes 1 and 2) mice. Furthermore, MMP-9 mRNA was increased in TR$\beta^{PV/PV}$ mice (Fig. 5Bb, bar 2) but not WT-PTU mice (bar 3), as compared with WT mice (bar 1). Taken together, the results indicate that PV, acting via integrins-Src-FAK-p38 MAPK-ATF2 signaling, increases the expression of MMP-9 to promote invasion and metastasis of thyroid tumor cells of TR$\beta^{PV/PV}$ mice.

In addition, p38 MAPK-ATF2 signaling is also activated by upstream growth factors (32). We focused our study on TGFβ because previously it was reported to increase the expression of integrin $\alpha V\beta 3$ in cells (29). In the present study, we also found increased expression of integrin $\alpha V\beta 3$ at the protein level in the thyroid of TR$\beta^{PV/PV}$ but not WT-PTU mice (see Fig. 3C, c and d,). Indeed, Western blot analysis shows that TGFβ (Fig. 5Ca, lanes 3 and 4) was elevated in TR$\beta^{PV/PV}$ mice but was lower in WT-PTU mice (lanes 5 and 6), as compared with WT mice (lanes 1 and 2). Moreover, the expression of TGFβ receptor type 1 (TGFβR1) was markedly increased in TR$\beta^{PV/PV}$ mice (Fig. 5Cb, lanes 3 and 4), as compared with WT (Fig. 5Cb, lanes 1 and 2) and WT-PTU mice (Fig. 5Cb, lanes 5 and 6). Together with the increased Grb2 (see Fig. 4Ag) associated with activated FAK, these results indicate that PV-induced activation of TGFβ-TGFβR1 signaling converges with integrin-Src-FAK-p38 MAPK-ATF2-MMP-9 to promote tumor cells invasion and metastasis.

Discussion

TSH has long been known as a major stimulator of thyrocyte proliferation. Whether it is an initiator of thyroid carcinogenesis, however, remains controversial. The use of TR$\beta^{PV/PV}$ mice with TSHR or without TSHR allows us to clarify this issue *in vivo*. Here we show that TR$\beta^{PV/PV}$ mice deficient in TSHR exhibited impaired thyroid growth due to the lack of TSH/TSHR proliferation signal and showed no signs of cancer (Fig. 6A). WT-PTU mice, having a 9.1-fold higher serum TSH concentration than TR$\beta^{PV/PV}$ mice, had aberrant thyroid growth but did not

Downloaded from https://academic.oup.com/endo/article/151/4/1929/2456740 by guest on 20 August 2022

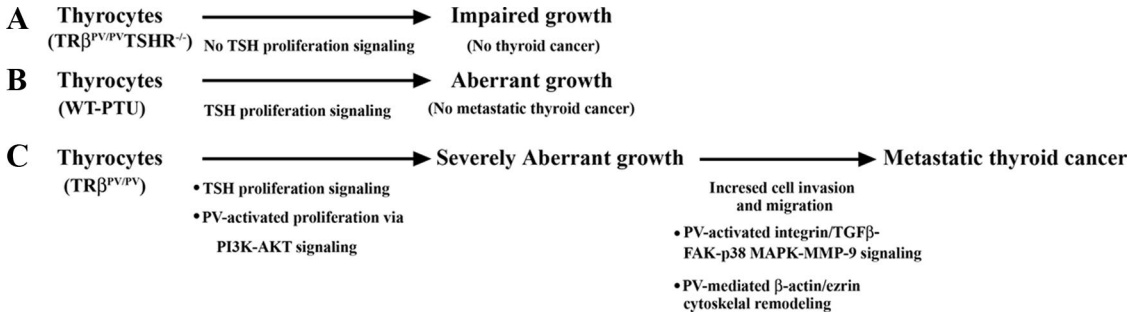

FIG. 6. Growth and metastasis in thyroid carcinogenesis. TR$\beta^{PV/PV}$TSHR$^{-/-}$, WT-PTU, and TR$\beta^{PV/PV}$ mice all have highly elevated serum TSH levels (see text). A, The thyroid of TR$\beta^{PV/PV}$ mice exhibited impaired growth in the absence of TSH proliferation signals due to the lack of TSHR. B, In WT-PTU mice, persistent TSH proliferation signaling resulted in aberrant thyroid growth without manifestation of metastatic thyroid cancer. C, In addition to TSH proliferation signaling, PV activated PI3K-AKT to further promote cell growth. In proliferating cells, PV further activated p38 MAPK phosphorylation cascades to increase the expression of MMPs such as MMP-9 and remodeled β-actin- and ezrin-associated cytoskeletal structures to facilitate cell migration and invasion.

develop metastatic thyroid cancer (Fig. 6B). Thus, these observations indicate that aberrant growth is a prerequisite, but is not sufficient, for the development of metastatic thyroid carcinoma. The occurrence of metastatic thyroid carcinoma requires additional genetic changes (such as PV) (Fig. 6C) that empower the hyperplastic cells to invade and metastasize.

In TR$\beta^{PV/PV}$ mice, the additional genetic change needed to empower hyperplastic thyrocytes to become invading tumor cells is a mutated TRβ gene (Fig. 6C). PV acted not only to further stimulate thyrocyte proliferation by amplifying the TSH-TSHR cross-signaling with AKT-mTOR-p70^{S6K} via direct activation of PI3K (Fig. 3B) (8) but also to activate the pathways that lead to increasing cell motility and invasion. Multiple mechanisms by which PV acted to affect the regulators and effectors involved in cell adhesion, motility, and migration were identified. PV functioned to increase the protein abundance of integrins $\alpha5$, αV, $\beta1$, and $\beta3$ and their ligand fibronectin as well as the cytoskeletal proteins actin and ezrin. PV activated cSrc by increasing its phosphorylation (Y416), which in turn activated FAK by increasing phosphorylation on several tyrosine sites. PV also recruited integrins $\alpha5$ and $\beta1$ and FAK to form complexes to transduce signals from ECM and TGFβ proteins via the p38 MAPK phosphorylation cascade to increase the expression of MMP-9 at the mRNA and protein levels (Fig. 5B). Furthermore, PV formed complexes with actin and ezrin, which are linked to FAK as components of adhesion focal contacts (25). The association of PV with FAK/actin/ezrin could remodel the cytoskeletal structure to facilitate migratory capabilities of tumor cells. Thus, PV acted via multiple mechanisms to enable hyperplastic tumor cells to migrate, invade, and metastasize.

The expression of FAK in 30 paired normal and malignant human thyroid specimens have been analyzed (33). The highest levels of FAK were seen in follicular carcinomas and tumors associated with distant metastatic foci. In contrast, neoplastic thyroid tissues with limited invasive potential, such as papillary carcinomas, follicular adenomas, and other nonmalignant thyroid lesions, showed minimal FAK expression (33). FAK has been proposed to be an invasion marker. Consistent with these observations, the present study elucidated the key role of FAK in the fibronectin-integrin-Src-FAK-p38 MAPK signaling that could promote metastatic follicular thyroid carcinogenesis. This pathway has provided novel therapeutic opportunities for the treatment of thyroid cancer. Indeed, in a recent study, an inhibitor of Src, AZD0530, was reported to inhibit the growth and invasion of four of five thyroid cancer cell lines, and the study found that high levels of p-FAK-Y861 correlate with AZD0530 sensitivity (34). These results support the idea that the Src-FAK complex represents a promising therapeutic strategy for patients with advanced thyroid cancer. Moreover, a novel FAK inhibitor, TAE226, has been shown to induce apoptosis in breast cancer cells (35) and another inhibitor, PF-562,271, was found to block tumorigenesis in breast, pancreatic, and prostate cells (36). Thus, TR$\beta^{PV/PV}$ mice could be used as a preclinical mouse model to test the effectiveness of the inhibitors of Src-FAK and other targets in the fibronectin-integrin-Src-FAK-p38 MAPK pathway in the treatment of follicular thyroid cancer.

Currently there are no reported patients with homozygous mutations of the TRβ gene to assess whether such patients, similar to TR$\beta^{PV/PV}$ mice, could develop follicular thyroid cancer. Nonetheless, the similarity with human follicular thyroid cancer in the patterns of pathological progression, cytopathological characteristics, and frequency of metastasis has made the TR$\beta^{PV/PV}$ mouse a unique model for dissecting molecular genetics and mechanisms of carcinogenesis of the thyroid (7, 37). Evidence has been accumulating to indicate that wild-type TRβ functions as a tumor suppressor (38, 39) and that somatic mutations of TRβ leading to the loss of its suppressor

Downloaded from https://academic.oup.com/endo/article/151/4/1929/2456740 by guest on 20 August 2022

functions are involved in the development of several types of human cancers (40).

The present study has provided several lines of evidence to indicate that aberrant growth of follicular cells is a prerequisite, but is not sufficient, for the development of metastatic FTC. Two or more additional genetic changes, destined to alter ECM proteins and/or regulators/effectors of signaling pathways in cell adhesion, motility, and migration, are required to bring about the metastatic phenotype. Thus, the present study suggests that growth and metastasis are two processes in the carcinogenesis of the thyroid. In the TR$\beta^{PV/PV}$ mouse, PV has met the necessary dual functions to induce metastatic thyroid carcinoma. PV acts to elevate serum TSH via dysregulation of the pituitary-thyroid axis, thus providing constitutive proliferation signals of thyrocytes to proliferate in the life of mice. In addition, PV, via nucleus-initiated transcriptional regulation as well as nongenomic actions (41), acts as an oncogene to alter cellular expression and activity of ECM, adhesion, and migration for tumor cells to invade.

This molecular model of growth and metastasis learned from the TR$\beta^{PV/PV}$ mouse could be extended to understand the mechanisms of carcinogenesis of human thyroid cancers. This molecular model is consistent with the clinical observations that higher TSH is associated with extrathyroidal extension of disease but not with distant metastases (42). But higher TSH values are associated with an increased risk of thyroid cancer because TSH increases thyroid growth (1, 43). Thus, goiters resulting from growth signals from either TSH or other aberrant stimuli could remain benign. However, additional genetic alterations involved changing cellular behaviors in adhesion, motility, and migration would need to occur for eventual metastasis because these abnormal clones continue to proliferate and expand. One critical issue for future research is to elucidate what these genetic changes are in human FTC and identify molecular targets for treatment. In view of the lessons learned from studies in TR$\beta^{PV/PV}$ mice, agents and drugs that could inhibit and block aberrant thyrocyte proliferation might be considered as a first-line preventive strategy for metastatic FTC.

Acknowledgments

Address all correspondence and requests for reprints to: Sheue-yann Cheng, Ph.D., Laboratory of Molecular Biology, National Cancer Institute, 37 Convent Drive, Room 5128, Bethesda, Maryland 20892-4264. E-mail: chengs@mail.nih.gov.

This work was supported by the Intramural Research Program of National Institutes of Health, National Cancer Institute, and Center for Cancer Research.

Disclosure Summary: The authors have nothing to disclose.

References

1. **Marians RC, Ng L, Blair HC, Unger P, Graves PN, Davies TF** 2002 Defining thyrotropin-dependent and -independent steps of thyroid hormone synthesis by using thyrotropin receptor-null mice. Proc Natl Acad Sci USA 99:15776–15781
2. **Haymart MR, Repplinger DJ, Leverson GE, Elson DF, Sippel RS, Jaume JC, Chen H** 2008 Higher serum thyroid stimulating hormone level in thyroid nodule patients is associated with greater risks of differentiated thyroid cancer and advanced tumor stage. J Clin Endocrinol Metab 93:809–814
3. **O'Sullivan C, Barton CM, Staddon SL, Brown CL, Lemoine NR** 1991 Activating point mutations of the gsp oncogene in human thyroid adenomas. Mol Carcinog 4:345–349
4. **Parrilla R, Mixson AJ, McPherson JA, McClaskey JH, Weintraub BD** 1991 Characterization of seven novel mutations of the c-erbAβ gene in unrelated kindreds with generalized thyroid hormone resistance. Evidence for two "hot spot" regions of the ligand binding domain. J Clin Invest 88:2123–2130
5. **Weiss RE, Refetoff S** 2000 Resistance to thyroid hormone. Rev Endocr Metab Disord 1:97–108
6. **Kaneshige M, Kaneshige K, Zhu X, Dace A, Garrett L, Carter TA, Kazlauskaite R, Pankratz DG, Wynshaw-Boris A, Refetoff S, Weintraub B, Willingham MC, Barlow C, Cheng S** 2000 Mice with a targeted mutation in the thyroid hormone β receptor gene exhibit impaired growth and resistance to thyroid hormone. Proc Natl Acad Sci USA 97:13209–13214
7. **Suzuki H, Willingham MC, Cheng SY** 2002 Mice with a mutation in the thyroid hormone receptor β gene spontaneously develop thyroid carcinoma: a mouse model of thyroid carcinogenesis. Thyroid 12:963–969
8. **Kim CS, Vasko VV, Kato Y, Kruhlak M, Saji M, Cheng SY, Ringel MD** 2005 AKT activation promotes metastasis in a mouse model of follicular thyroid carcinoma. Endocrinology 146:4456–4463
9. **Furuya F, Hanover JA, Cheng SY** 2006 Activation of phosphatidylinositol 3-kinase signaling by a mutant thyroid hormone β receptor. Proc Natl Acad Sci USA 103:1780–1785
10. **Ying H, Furuya F, Zhao L, Araki O, West BL, Hanover JA, Willingham MC, Cheng SY** 2006 Aberrant accumulation of PTTG1 induced by a mutated thyroid hormone β receptor inhibits mitotic progression. J Clin Invest 116:2972–2984
11. **Zimonjic DB, Kato Y, Ying H, Popescu NC, Cheng SY** 2005 Chromosomal aberrations in cell lines derived from thyroid tumors spontaneously developed in TRβPV/PV mice. Cancer Genet Cytogenet 161:104–109
12. **Guigon CJ, Zhao L, Willingham MC, Cheng SY** 2009 PTEN deficiency accelerates tumour progression in a mouse model of thyroid cancer. Oncogene 28:509–517
13. **Furumoto H, Ying H, Chandramouli GV, Zhao L, Walker RL, Meltzer PS, Willingham MC, Cheng SY** 2005 An unliganded thyroid hormone β receptor activates the cyclin D1/cyclin-dependent kinase/retinoblastoma/E2F pathway and induces pituitary tumorigenesis. Mol Cell Biol 25:124–135
14. **Garcia-Jiménez C, Santisteban P** 2007 TSH signalling and cancer. Arq Bras Endocrinol Metab 51:654–671
15. **Suh JM, Song JH, Kim DW, Kim H, Chung HK, Hwang JH, Kim JM, Hwang ES, Chung J, Han JH, Cho BY, Ro HK, Shong M** 2003 Regulation of the phosphatidylinositol 3-kinase, Akt/protein kinase B, FRAP/mammalian target of rapamycin, and ribosomal S6 kinase 1 signaling pathways by thyroid-stimulating hormone (TSH) and stimulating type TSH receptor antibodies in the thyroid gland. J Biol Chem 278:21960–21971
16. **De Gregorio G, Coppa A, Cosentino C, Ucci S, Messina S, Nicolussi A, D'Inzeo S, Di Pardo A, Avvedimento EV, Porcellini A** 2007 The p85 regulatory subunit of PI3K mediates TSH-cAMP-PKA growth and survival signals. Oncogene 26:2039–2047
17. **Ensinger C, Obrist P, Bacher-Stier C, Mikuz G, Moncayo R,**

Downloaded from https://academic.oup.com/endo/article/151/4/1929/2456740 by guest on 20 August 2022

Riccabona G 1998 β1-Integrin expression in papillary thyroid carcinoma. Anticancer Res 18:33–40
18. **Dahlman T, Grimelius L, Wallin G, Rubin K, Westermark K** 1998 Integrins in thyroid tissue: upregulation of α2β1 in anaplastic thyroid carcinoma. Eur J Endocrinol 138:104–112
19. **Hoffmann S, Maschuw K, Hassan I, Reckzeh B, Wunderlich A, Lingelbach S, Zielke A** 2005 Differential pattern of integrin receptor expression in differentiated and anaplastic thyroid cancer cell lines. Thyroid 15:1011–1020
20. **Illario M, Cavallo AL, Monaco S, Di Vito E, Mueller F, Marzano LA, Troncone G, Fenzi G, Rossi G, Vitale M** 2005 Fibronectin-induced proliferation in thyroid cells is mediated by αvβ3 integrin through Ras/Raf-1/MEK/ERK and calcium/CaMKII signals. J Clin Endocrinol Metab 90:2865–2873
21. **Ramsay AG, Marshall JF, Hart IR** 2007 Integrin trafficking and its role in cancer metastasis. Cancer Metastasis Rev 26:567–578
22. **Brunton VG, Frame MC** 2008 Src and focal adhesion kinase as therapeutic targets in cancer. Curr Opin Pharmacol 8:427–432
23. **McLean GW, Carragher NO, Avizienyte E, Evans J, Brunton VG, Frame MC** 2005 The role of focal-adhesion kinase in cancer—a new therapeutic opportunity. Nat Rev Cancer 5:505–515
24. **Schlaepfer DD, Hunter T** 1996 Evidence for *in vivo* phosphorylation of the Grb2 SH2-domain binding site on focal adhesion kinase by Src-family protein-tyrosine kinases. Mol Cell Biol 16:5623–5633
25. **Mitra SK, Hanson DA, Schlaepfer DD** 2005 Focal adhesion kinase: in command and control of cell motility. Nat Rev Mol Cell Biol 6:56–68
26. **Angers-Loustau A, Hering R, Werbowetski TE, Kaplan DR, Del Maestro RF** 2004 SRC regulates actin dynamics and invasion of malignant glial cells in three dimensions. Mol Cancer Res 2:595–605
27. **Avizienyte E, Keppler M, Sandilands E, Brunton VG, Winder SJ, Ng T, Frame MC** 2007 An active Src kinase-β-actin association is linked to actin dynamics at the periphery of colon cancer cells. Exp Cell Res 313:3175–3188
28. **Yu Y, Khan J, Khanna C, Helman L, Meltzer PS, Merlino G** 2004 Expression profiling identifies the cytoskeletal organizer ezrin and the developmental homeoprotein Six-1 as key metastatic regulators. Nat Med 10:175–181
29. **Pechkovsky DV, Scaffidi AK, Hackett TL, Ballard J, Shaheen F, Thompson PJ, Thannickal VJ, Knight DA** 2008 Transforming growth factor β1 induces αvβ3 integrin expression in human lung fibroblasts via a β3 integrin-, c-Src-, and p38 MAPK-dependent pathway. J Biol Chem 283:12898–12908
30. **Kim ES, Sohn YW, Moon A** 2007 TGF-β-induced transcriptional activation of MMP-2 is mediated by activating transcription factor (ATF)2 in human breast epithelial cells. Cancer Lett 252:147–156
31. **Dziembowska M, Danilkiewicz M, Wesolowska A, Zupanska A, Chouaib S, Kaminska B** 2007 Cross-talk between Smad and p38 MAPK signalling in transforming growth factor β signal transduction in human glioblastoma cells. Biochem Biophys Res Commun 354:1101–1106
32. **Cuenda A, Rousseau S** 2007 p38 MAP-kinases pathway regulation, function and role in human diseases. Biochim Biophys Acta 1773: 1358–1375
33. **Owens LV, Xu L, Dent GA, Yang X, Sturge GC, Craven RJ, Cance WG** 1996 Focal adhesion kinase as a marker of invasive potential in differentiated human thyroid cancer. Ann Surg Oncol 3:100–105
34. **Schweppe RE, Kerege AA, French JD, Sharma V, Grzywa RL, Haugen BR** 2009 Inhibition of Src with AZD0530 reveals the Src-focal adhesion kinase complex as a novel therapeutic target in papillary and anaplastic thyroid cancer. J Clin Endocrinol Metab 94:2199–2203
35. **Golubovskaya VM, Virnig C, Cance WG** 2008 TAE226-induced apoptosis in breast cancer cells with overexpressed Src or EGFR. Mol Carcinog 47:222–234
36. **Roberts WG, Ung E, Whalen P, Cooper B, Hulford C, Autry C, Richter D, Emerson E, Lin J, Kath J, Coleman K, Yao L, Martinez-Alsina L, Lorenzen M, Berliner M, Luzzio M, Patel N, Schmitt E, LaGreca S, Jani J, Wessel M, Marr E, Griffor M, Vajdos F** 2008 Antitumor activity and pharmacology of a selective focal adhesion kinase inhibitor, PF-562,271. Cancer Res 68:1935–1944
37. **Cheng SY** 2005 Thyroid hormone receptor mutations and disease: beyond thyroid hormone resistance. Trends Endocrinol Metab 16: 176–182
38. **Martínez-Iglesias O, Garcia-Silva S, Tenbaum SP, Regadera J, Larcher F, Paramio JM, Vennström B, Aranda A** 2009 Thyroid hormone receptor β1 acts as a potent suppressor of tumor invasiveness and metastasis. Cancer Res 69:501–509
39. **García-Silva S, Aranda A** 2004 The thyroid hormone receptor is a suppressor of ras-mediated transcription, proliferation, and transformation. Mol Cell Biol 24:7514–7523
40. **Cheng SY** 2003 Thyroid hormone receptor mutations in cancer. Mol Cell Endocrinol 213:23–30
41. **Furuya F, Lu C, Guigon CJ, Cheng SY** 2009 Nongenomic activation of phosphatidylinositol 3-kinase signaling by thyroid hormone receptors. Steroids 74:628–634
42. **Haymart MR, Glinberg SL, Liu J, Sippel RS, Jaume JC, Chen H** 2009 Higher serum TSH in thyroid cancer patients occurs independent of age and correlates with extrathyroidal extension. Clin Endocrinol (Oxf) 71:434–439
43. **Jonklaas J, Nsouli-Maktabi H, Soldin SJ** 2008 Endogenous thyrotropin and triiodothyronine concentrations in individuals with thyroid cancer. Thyroid 18:943–952

Downloaded from https://academic.oup.com/endo/article/151/4/1929/2456740 by guest on 20 August 2022